pyramidal.[10] In these cases, however, the axial ligand was not a strong donor such as nitrogen but, rather, a weakly coordinating anion or solvent molecule. Similar results were found for imidazolate-bridged dicopper(II) complexes of large Schiff base macrocycles[25] having only water or perchlorate anions in the axial sites. Trigonal bipyramidal geometry is somewhat unusual for copper(II) complexes unless the ligand system requires it. For example, tren, bipyridine, and *o*-phenanthroline often give trigonal-bipyramidal copper(II) complexes.[27,31] The macrocycles A and A′ were expected to provide square-planar coordination geometries, possibly with weakly bound axial ligands, as found for $[Cu_2(TMDT)_2(im)]^{3+}$. Such is presumably the case for $[Cu_2(im)\subset A'](ClO_4)_3\cdot H_2O$, although the structure could not be determined. Although trigonal-bipyramidal structures occur in the solid state for $[Cu_2(im)(imH)_2\subset A]^{3+}$ and $[Cu_2(im)(MeIm)_2\subset A']^{3+}$, in solution the coordinated imidazoles are most likely replaced by two water molecules to form square-pyramidal copper(II) centers.[13,23]

Acknowledgment. This work was supported at Columbia University by NIH Research Grant No. GM-16449 from the National Institute of General Medical Sciences and by Grant No. CHE 81-09390 from the National Science Foundation.

Registry No. 1, 69470-57-1; 2, 89016-78-4; $[Cu_2(im)\subset A'](ClO_4)_3$, 76096-70-3.

Supplementary Material Available: Tables S1–S7 reporting observed and calculated structure factor amplitudes, hydrogen atom positional parameters, atomic thermal parameters, and ligand torsion angles (17 pages). Ordering information is given on any current masthead page.

---

[31] Hathaway, G. J.; Billing, D. E. *Coord. Chem. Rev.* **1970**, *5*, 5143.

Contribution from the Department of Chemistry,
University of California, Berkeley, California 94720

Synthetic, Structural, and Physical Studies of Titanium Complexes of Catechol and 3,5-Di-*tert*-butylcatechol

BRANDAN A. BORGIAS, STEPHEN R. COOPER, YUN BAI KOH, and KENNETH N. RAYMOND*

Received August 16, 1983

Catechol ligands are found in biologically important metal complexing agents and have a remarkable affinity for metal ions in high oxidation states or with high charge/radius ratios. The coordination chemistry of titanium with catechol (H_2cat) and 3,5-di-*tert*-butylcatechol (H_2DTBC) is described, and the preparation and characterization of several types of complexes are reported. The structures of the representative compounds $[Et_3NH]_2[Ti(cat)_3]$ (**2**) (Ia, with $a = 9.431$ (1) Å, $b = 32.634$ (4) Å, $c = 10.055$ (1) Å, and $\beta = 100.07$ (1)°; $Z = 4$; $\rho_{calcd} = 1.257$, $\rho_{obsd} = 1.25$ g cm^{-3}; $R_w = 3.79\%$), $K_4[TiO(cat)_2]_2\cdot 9H_2O$ (**4**) ($I2/a$, with $a = 20.602$ (1) Å, $b = 6.237$ (1) Å, $c = 28.099$ (2) Å, and $\beta = 102.37$ (1)°; $Z = 4$; $\rho_{calcd} = 1.655$ g cm^{-3}; $R_w = 6.4\%$), and $[Et_3NH]_2[Ti(DTBC)_2(HDTBC)]_2\cdot 2CHCl_3$ (**5**) ($P\bar{1}$, with $a = 14.369$ (1) Å, $b = 14.617$ (1) Å, $c = 15.330$ (2) Å, $\alpha = 62.12$ (1)°, $\beta = 81.85$ (1)°, and $\gamma = 70.35$ (1)°; $Z = 1$; $\rho_{calcd} = 1.154$ g cm^{-3}; $R_w = 8.7\%$) have been determined by single-crystal X-ray diffraction. The complex anions of **4** and **5** are dimers with oxo and catecholato oxygen bridging groups, respectively. The $Ti(cat)_3^{2-}$ complex in **2** is pseudooctahedral with an average Ti–O bond length of 1.966 (27) Å. The average trigonal twist angle (0° for trigonal prism, 60° for the octahedron) is 43.5°. Strong hydrogen bonds from the cations to the catecholate oxygens perturb the geometry significantly from the D_3 ideal symmetry. The bis(μ-oxo) dimer $[TiO(cat)_2]_2^{4-}$ in **4** lies on an inversion center with nearly C_{2h} molecular symmetry. The Ti_2O_2 unit has an internal O–Ti–O bond angle of 82° and a Ti–Ti separation of 2.82 Å. The Ti–O catechol bonds trans to the oxide anions are 0.061 Å longer (2.051 (19) Å vs. 1.990 (3) Å) than the cis bonds. In contrast, the $[Ti(DTBC)_2(HDTBC)]_2^{2-}$ anion of **5** is a dimer, which contains both monoanionic and dianionic catecholate ligands, with crystallographic inversion symmetry. The monoanion ($HDTBC^-$) is monodentate, but one of the bidentate dianion ($DTBC^{2-}$) oxygen atoms is coordinated to both metal anions to form a dimeric complex of hexacoordinate Ti(IV). The average Ti–O bridge bonds are longer (2.060 (19) Å vs. 1.887 (2) Å) than the bonds trans to them. The monodentate catechol Ti–O bond distance is 1.936 (2) Å. For each of the structural types infrared and optical spectra are reported. For the $Ti(cat)_3^{2-}$ complex there is a hydrolysis reaction that takes place to form the $[TiO(cat)_2]^{2-}$ dimer above pH 12. The cyclic voltammetry of $Ti(cat)_3^{2-}$ shows a reversible reduction wave corresponding to a standard reduction potential (NHE) of −1.14 V. This remarkable shift of the standard Ti(IV)/Ti(III) reduction potential (0.099 V for $Ti(OH)_2^{2+}/Ti^{3+}$ in acid) is due to the enormous stability of the $Ti(cat)_3^{2-}$ complex.

Introduction

Catechol (1,2-dihydroxybenzene) is a powerful, bidentate chelating agent which has a particular affinity for metal ions that exhibit high oxidation states or high charge to metal ion radius ratios.[1] In biology, catechol functional groups are found in certain siderophores (microbial iron-chelating agents).[2] We have incorporated catechol ligands in the synthesis of sequestering agents that are designed to be specific for iron(III) or actinide(IV) metal ions.[3] This has led us to a general interest in the coordination chemistry of simple catechols. A previous paper reported the solution equilibria and characterization of several vanadium catechol complexes.[4] In this paper the coordination chemistry of catechol and 3,5-di-*tert*-butylcatechol (H_2DTBC) with titanium is explored and the structures of three representative complexes are reported.

In their pioneering study of metal–catecholate chemistry, Rosenheim and co-workers reported the synthesis of $[NH_4]_2[Ti(cat)_3]\cdot H_2O$.[5] A subsequent paper reported the resolution of the anion into its enantiomeric forms.[6] Rosen-

---

[1] Kappel, M. J.; Raymond, K. N. *Inorg. Chem.* **1982**, *21*, 3437.

[2] Raymond, K. N.; Carrano, C. J. *Acc. Chem. Res.* **1979**, *12*, 183.

[3] Raymond, K. N.; Harris, W. R.; Carrano, C. J.; Weitl, F. L. *ACS Symp. Ser.* **1980**, *No. 140*, 313.

[4] Cooper, S. R.; Koh, Y. B.; Raymond, K. N. *J. Am. Chem. Soc.* **1982**, *104*, 5092.

[5] Rosenheim, A.; Sorge, O. *Chem. Ber.* **1920**, *53*, 932.

[6] Rosenheim, A.; Raibmann, B.; Schendel, G. *Z. Anorg. Allg. Chem.* **1931**, *196*, 160.

heim noted with evident surprise that catechol solutions are capable of dissolving hydrous titanium oxides (which are relatively intractable). This reflects the enormous affinity of catechol for strong Lewis acids such as Ti(IV). Analytical application of this Ti(IV)–catechol system appears to have been limited largely to acidic media, presumably because of concern about hydrolysis and polymerization of Ti(IV). In 1963 Sommer placed analytical use of the titanium–catecholate system on a firm basis with his studies of the solution equilibria that occur at low pH.[7]

The remarkably high formation constants of complexes formed between catechol anion and cations such as Fe(III) and Ce(IV)[3] give rise to large changes in the redox potentials, hydrolytic reactions, and other equilibria of the complex species. Indeed, although complexes of vanadium(IV) in aqueous solution invariably contain the vanadyl (VO^{2+}) ion, the catechol complex $V(cat)_3^{2-}$ is octahedral.[4] This leads to the expectation that the aqueous chemistry of Ti(IV) catechol complexes should be profoundly different from the usual chemistry of the Ti(IV) ion. We report here the solution chemistry and electrochemical behavior of $[Ti(cat)_3]^{2-}$, as well as the isolation and X-ray crystal structures of $[Et_3NH]_2[Ti(cat)_3]$ (**2**), and two dimeric hydrolysis products: a bis(μ-oxo) dimer, $K_4[TiO(cat)_2]_2 \cdot 9H_2O$ (**4**), and a catechol-bridged dimer, $[Et_3NH]_2[Ti(DTBC)_2(HDTBC)]_2 \cdot 2CHCl_3$ (**5**).

Experimental Section

Chemicals. Catechol (Crown-Zellerbach) and 3,5-di-*tert*-butylcatechol (Aldrich) were purified by treating with activated charcoal and then recrystallizing from benzene and *n*-hexane, respectively. $TiCl_4$ (Alfa) was distilled (bp 134 °C) prior to use. All other chemicals were reagent grade and were used as received. Standard Schlenk techniques under argon atmosphere were used for all preparations to prevent the air oxidation of the catechol ligands under the basic conditions of the syntheses.

Physical Measurements. Infrared spectra were recorded as KBr pellets on a Perkin-Elmer 283 grating spectrometer calibrated with polystyrene. Cyclic voltammetry was performed with a hanging mercury drop electrode (HMDE) as previously described.[8] A stirred mercury pool electrode was used in the place of the HMDE for preparative controlled-potential reduction experiments. All electrochemical measurements were performed on deoxygenated solutions under argon. All potentials are reported vs. the saturated calomel reference electrode (SCE) and are uncorrected for liquid-junction potentials. Optical measurements were performed at ambient temperatures on a Cary 118 or Hewlett-Packard 8450A spectrophotometer with quartz cuvettes. Microanalyses were performed by the Microanalytical Laboratory, Department of Chemistry, University of California, Berkeley.

Synthesis. $[NH_4]_2[Ti(cat)_3] \cdot 2H_2O$ (1). A 10.0-g (53-mmol) sample of $TiCl_4$ in 20 mL of 1 M HCl was stirred into a deoxygenated solution containing 20.0 g (180 mmol) of catechol dissolved in 80 mL of hot 15% NH_4OH. The mixture was stirred at 80 °C for 1 h and the resultant deep red solution cooled to room temperature. The air-stable red crystals that formed upon cooling were collected by filtration, washed twice with 10% NH_4OH and once with absolute EtOH, and air-dried; yield 16.2 g (71%). Rosenheim et al. report isolating the monohydrate salt from a similar procedure.[6] Our analytical and crystalline data (vide infra) support the present formulation of a dihydrate for the freshly prepared, crystalline material.

Anal. Calcd for $C_{18}H_{24}N_2O_8Ti$: C, 48.66; H, 5.44; N, 6.30; Ti, 10.78. Found: C, 48.29; H, 5.43; N, 6.26; Ti, 10.6. The complex was recrystallized from a hot 2 M NH_4Cl solution that was allowed to cool slowly to room temperature. This yielded well-formed hexagonal rods that were dichroic (red/yellow).

$[Et_3NH]_2[Ti(cat)_3]$ (2). This was prepared in a manner analogous to that for the ammonium salt and was recrystallized from an $EtOH/H_2O$ (~20/1) solution that was allowed to cool slowly to 5 °C. This yielded blocky red crystals from which fragments were cleaved for X-ray diffraction measurements.

Anal. Calcd for $C_{30}H_{44}N_2O_6Ti$: C, 62.49; H, 7.69; N, 4.86. Found: C, 62.41; H, 7.64; N, 4.80.

$K_4[TiO(cat)_2]_2 \cdot 2H_2O$ (3). A 1.5-g (3.4-mmol) sample of (**1**) was refluxed in 10 mL of 1 M aqueous KOH for 30 min. After the solution was concentrated to 5 mL, a 30-mL portion of absolute EtOH was added and the resulting yellow solution was stirred for 10 min. During this time yellow crystals deposited. These were filtered, rinsed with absolute EtOH, and dried in a stream of argon; yield 0.60 g (41%).

Anal. Calcd for $C_{12}H_{10}O_6TiK_2$: C, 38.38; H, 2.66; Ti, 12.76. Found: C, 38.74; H, 3.15; Ti, 12.4.

Recrystallization from 0.1 M KOH yielded crystals suitable for X-ray diffraction studies, isolated as $K_4[TiO(cat)_2]_2 \cdot 9H_2O$ (**4**).

$[Et_3NH]_2[Ti(DTBC)_2(HDTBC)]_2$ (5). A solution containing 3.6 g (1.6 mmol) of $Ti(OEt)_4$[9] dissolved in 5 mL of hexane was mixed with 1.1 g (5.0 mmol) of 3,5-di-*tert*-butylcatechol in 5 mL of hexane and 2 mL (14 mmol) of Et_3N. The solution was boiled under reflux overnight. The resulting red crystals were filtered, washed with absolute EtOH, and air-dried; yield 1.1 g (85%).

Anal. Calcd for $C_{48}H_{77}NO_6Ti$: C, 71.02; H, 9.37; N, 1.73; Ti, 5.91. Found: C, 70.86; H, 9.36; N, 1.71; Ti, 5.98.

Slow evaporation of a chloroform solution under argon atmosphere yielded good crystals, isolated as a chloroform solvate.

X-ray Diffraction. Compound **1** gave well-formed crystals that proved to be intractable. Precession photographs indicated $6/m$ Laue symmetry, with no systematic absences. This results in an ambiguity for the space group (either $P6$, $P\bar{6}$, or $P6/m$). The density, 1.35 g/mL (measured by flotation in $CHCl_3$/toluene), and the cell volume, 2151 Å^3, indicated that $Z = 4$. This requires the Ti atoms to occupy special positions (presumably the threefold positions). A redundant data set was collected (including both sixfold and mirror-related reflections). After averaging of the data it was discovered that the reflections related by the mirror plane were only in moderate agreement (~10%). However, when the reflections were averaged with only $\bar{3}$ symmetry assumed, the resulting agreement factor was 2.7%. Thus the actual Laue group appears to be $P\bar{3}$. However, no satisfactory, ordered structure was obtained and the crystal was abandoned in favor of the triethylammonium salt, **2**.

Crystal fragments of compound **2** were cleaved from larger blocks. These were mounted on glass fibers with epoxy cement. Crystals of **4** and **5** with suitable dimensions were placed in glass capillaries filled with the mother liquors from which they were grown. The capillaries were sealed with epoxy cement. After brief photographic examination, the crystals were aligned on an Enraf-Nonius CAD 4 automated diffractometer. Setting angles of 24 high-angle reflections were used to determine accurate cell constants (Table I). Nonstandard body-centered (I) cells were chosen for data collection of **2** and **4**, since for both crystals this setting gave much less obtuse cells than the standard C-centered monoclinic cells. Intensity data were collected by the θ–2θ scan technique using monochromatic Mo Kα radiation. For compound **2** a redundant data set was collected for subsequent averaging. For each crystal three intensity standards and three orientation standards were monitored periodically. Compound **5** showed an isotropic decrease of 20% in the intensities of standard reflections over the period of data collection; correction for this decomposition was applied. An empirical absorption correction was applied to the data for **4** using ϕ scans near $\chi = 90°$. The raw data were processed as described elsewhere.[10] The redundant data for **2** ($+h,+k,\pm l$, $+h,-k,\pm l$) were averaged to yield 4428 unique data with an agreement factor for averaging (based on I) of 2.4%. Only reflections with $F_o^2 > 3\sigma(F_o^2)$ were used in the subsequent structure determination and refinement.

Structure Solution and Refinement. $[Et_3NH]_2[Ti(cat)_3]$. Since the amplitude distribution of normalized structure factors (E's) corresponded closely to an acentric distribution,[10] the space group Ia was chosen for initial structure analysis. Subsequent refinement of the structure confirmed this choice. The structure was solved by heavy-atom methods. Essentially all the hydrogen atoms were found following full anisotropic refinement of the non-hydrogen atoms. The amine protons were placed at the coordinates indicated by the difference Fourier map with $B = 5.0$ Å^2. All other hydrogen atoms were

---

(7) Sommer, L. *Collect. Czech. Chem. Commun.* **1963**, *28*, 2102.

(8) Cooper, S. R.; McArdle, J. V.; Raymond, K. N. *Proc. Natl. Acad. Sci. U.S.A.* **1978**, *75*, 3551.

(9) Prepared as previously described: Bradley, D. C.; Gaze, R.; Wardlaw, W. *J. Chem. Soc.* **1955**, 721.

(10) Eigenbrot, C. W., Jr.; Raymond, K. N. *Inorg. Chem.* **1982**, *21*, 2653.

Table I. Crystal Data

	$[Et_3NH]_2[Ti(cat)_3]$	$K_4[TiO(cat)_2]_2 \cdot 9H_2O$	$[Et_3NH]_2$-$[Ti(DTBC)_2(HDTBC)]_2 \cdot 2CHCl_3$
M_r	576.6	978.7	1862.9
space group	Ia^a	$I2/a^b$	$P\bar{1}$
a, Å	9.431 (1)	20.602 (1)	14.369 (1)
b, Å	32.634 (4)	6.237 (1)	14.617 (1)
c, Å	10.055 (1)	28.099 (2)	15.330 (2)
α, deg	90	90	62.12 (1)
β, deg	100.07 (1)	102.37 (1)	81.85 (1)
γ, deg	90	90	70.35 (1)
V, Å^3	3047.6	3536.6	2679.6
ρ_{calcd}, g/cm^3	1.257	1.655	1.154
ρ_{obsd}, g/cm^3	1.25		
Z	4	4	1
μ, cm^{-1}	3.17	11.6	3.49
cryst size, mm	0.42 × 0.33 × 0.28	0.45 × 0.35 × 0.23	0.44 × 0.40 × 0.23
no. of indep reflcns	4428^c	4039	12 279
2θ range, deg	3-60	3-55	3-55
no. of indep reflcns, $F_o^2 > 3\sigma(F_o^2)$	3602	3371	6722
R (%)	2.76	3.4	6.2
R_w (%)	3.79	6.4	8.7
GOF	1.30	1.86	2.07
no. of variables	351	222	541

[a] An alternate setting of Cc. [b] An alternate setting of $C2/c$. [c] After averaging 9327 reflections ($+h,\pm k,\pm l$).

Table II. Positional Parameters of $[Et_3NH]_2[Ti(cat)_3]$

atom	x	y	z	B_{eqv}, Å^{2a}	atom	x	y	z	B_{eqv}, Å^{2a}
Ti	0.000	0.12157 (1)	0.000	2.850 (4)	C25	−0.3955 (3)	0.22814 (7)	0.0379 (3)	4.64 (5)
O1	0.0838 (2)	0.08523 (5)	0.1455 (2)	3.84 (3)	C26	−0.3190 (2)	0.19575 (7)	0.1056 (2)	3.92 (4)
O2	0.1696 (2)	0.15410 (5)	0.0773 (2)	3.84 (3)	C31	−0.1085 (2)	0.06064 (6)	−0.1905 (2)	2.85 (3)
O3	−0.1364 (2)	0.14397 (4)	0.1034 (1)	3.45 (3)	C32	0.0217 (2)	0.07381 (6)	−0.2277 (2)	3.01 (3)
O4	−0.0782 (2)	0.16857 (4)	−0.1208 (1)	3.38 (3)	C33	0.0659 (2)	0.05741 (7)	−0.3403 (2)	3.75 (4)
O5	−0.1402 (1)	0.07888 (4)	−0.0785 (1)	3.08 (2)	C34	−0.0183 (3)	0.02772 (8)	−0.4160 (2)	4.34 (4)
O6	0.0935 (2)	0.10248 (5)	−0.1477 (2)	3.54 (3)	C35	−0.1441 (3)	0.01482 (8)	−0.3793 (2)	4.29 (5)
N1	0.0663 (2)	0.19328 (5)	−0.3169 (2)	3.44 (3)	C36	−0.1907 (2)	0.03125 (7)	−0.2666 (2)	3.74 (4)
N2	−0.4010 (2)	0.07101 (5)	0.0273 (2)	3.38 (3)	CN11	0.0287 (3)	0.23712 (7)	−0.3530 (2)	3.97 (4)
C11	0.1975 (3)	0.10029 (8)	0.2297 (2)	3.77 (4)	CN12	0.2195 (3)	0.18796 (8)	−0.2485 (3)	4.53 (5)
C12	0.2460 (2)	0.13853 (7)	0.1916 (2)	3.70 (4)	CN13	0.0307 (4)	0.16518 (8)	−0.4357 (3)	5.19 (6)
C13	0.3626 (3)	0.15743 (9)	0.2689 (3)	4.90 (5)	CN14	0.0546 (3)	0.26577 (8)	−0.2347 (3)	4.64 (5)
C14	0.4323 (3)	0.1373 (1)	0.3862 (3)	6.21 (7)	CN15	0.3288 (3)	0.2025 (1)	−0.3320 (4)	7.03 (7)
C15	0.3859 (4)	0.0998 (1)	0.4226 (3)	6.53 (8)	CN16	−0.1287 (5)	0.1594 (1)	−0.4784 (4)	8.16 (9)
C16	0.2670 (3)	0.0809 (1)	0.3444 (2)	5.26 (6)	CN21	−0.4523 (2)	0.02754 (7)	0.0049 (3)	4.12 (4)
C21	−0.2151 (2)	0.17600 (6)	0.0484 (2)	3.10 (3)	CN22	−0.3770 (3)	0.08281 (7)	0.1738 (2)	4.23 (4)
C22	−0.1849 (2)	0.18927 (6)	−0.0768 (2)	3.06 (3)	CN23	−0.4981 (3)	0.10168 (8)	−0.0549 (3)	4.57 (5)
C23	−0.2627 (3)	0.22135 (7)	−0.1446 (2)	4.06 (4)	CN24	−0.5948 (3)	0.01954 (9)	0.0494 (4)	6.66 (6)
C24	−0.3681 (3)	0.24073 (8)	−0.0849 (3)	4.66 (5)	CN25	−0.2677 (4)	0.0574 (1)	0.2613 (3)	6.54 (8)
					CN26	−0.5057 (4)	0.0963 (1)	−0.2031 (4)	6.89 (8)

[a] $B_{eqv} = \frac{4}{3}[a^2\beta_{11} + b^2\beta_{22} + c^2\beta_{33} + ab(\cos\gamma)\beta_{12} + ac(\cos\beta)\beta_{13} + bc(\cos\alpha)\beta_{23}]$.

assigned idealized positions, with a C–H distance of 0.95 Å, and isotropic temperature factors of $B + 1$ where B is the isotropic temperature factor corresponding to the geometric mean of the thermal motion of the carbon atoms to which they are bonded. Hydrogen atoms were included in structure factor calculations, but their parameters were not varied. A value of 0.04 was used for the parameter p in the weighting scheme,[10] and an extinction coefficient was refined in the final cycles to a value of 5.71×10^{-7} e^{-2}. The largest parameter shift in the last cycle was 7% of the associated standard deviation, and the final agreement factors were $R = 2.76\%$ and $R_w = 3.79\%$. The largest peak in the final difference Fourier was 0.32 e/Å^3, located near the Ti atom. Positional and thermal parameters are listed in Table II.[11]

$K_4[TiO(cat)_2]_2 \cdot 9H_2O$. The structure was solved by heavy-atom techniques. During the final stages of refinement, aromatic hydrogen atoms were assigned fixed, calculated positions, with $B = 5.0$ Å^2 and a C–H distance of 0.95 Å. A value of 0.06 was used for the parameter p in the weighting function. Refinement was terminated when positional and thermal parameters shifted no more than one-tenth of their standard deviations. Final agreement factors were $R = 3.4\%$ and $R_w = 6.4\%$. The final difference Fourier map showed no peaks greater than 0.38 e/Å^3. Positional and thermal parameters are listed in Table V.[11]

$[Et_3NH]_2[Ti(DTBC)_2(HDTBC)]_2 \cdot 2CHCl_3$. The structure was solved by the heavy-atom method. The *tert*-butyl groups at position 5 of the catechol rings were found to have large thermal motions. Inspection of the difference Fourier map did not indicate a well-resolved disorder. Instead it appears that these groups are essentially freely rotating. Ordinary anisotropic refinement is incapable of modeling such large thermal motions. Residual peaks of ~0.5 e/Å^3 were consistently found to occupy positions between the *tert*-butyl methyl carbons. Carbon atoms with 25% occupancy were placed at these idealized coordinates but not refined. The principal *tert*-butyl carbons were reduced to 75% occupancy and refined anisotropically. In the latter stages of refinement it became apparent that the monoprotonated catechol ligand was actually disordered about the O5–C31–C34 axis. This exchanges the *tert*-butyl groups at positions 3 and 5, and the partially occupied protonated oxygens at positions 2 (85%) and 6 (15%). This disordered model is substantiated by the fact the O6 atom forms credible hydrogen bonds in either position (O6···O1′ = 2.861 (2) Å, O1′···O6–C32 = 132.3 (2)°, O6a···O2 = 2.737 (2) Å, O2···O6a–C36 = 112.1 (1)°). Both protonic hydrogens (N–H and O6–H) were located in the difference Fourier map and were included

---

(11) See the statement at the end of this paper regarding supplementary tables, which include thermal parameters, calculated coordinates for hydrogen atoms, structure factor tables, and nonessential bond distances and angles.

Table V. Positional Parameters of $K_4[TiO(cat)_2]_2 \cdot 9H_2O$

atom	x	y	z	B_{eqv}, Å^{2a}	atom	x	y	z	B_{eqv}, Å^{2a}
Ti	0.74654 (2)	0.22385 (6)	0.19969 (1)	1.71 (1)	O10	0.75000 (0)	0.1805 (6)	0.00000 (0)	6.04 (9)
K1	0.74897 (3)	0.71242 (9)	0.11609 (2)	3.27 (1)	C11	0.84787 (11)	0.2265 (4)	0.14340 (8)	2.22 (4)
K2	0.86131 (3)	0.74068 (8)	0.27862 (2)	2.57 (1)	C12	0.85877 (10)	0.0358 (4)	0.17072 (8)	2.21 (4)
O1	0.79824 (8)	0.3483 (3)	0.15217 (6)	2.60 (3)	C13	0.90856 (12)	−0.1045 (5)	0.16491 (9)	3.02 (4)
O2	0.81735 (7)	0.0047 (3)	0.20136 (5)	2.39 (3)	C14	0.94819 (12)	−0.0548 (5)	0.13181 (9)	3.45 (4)
O3	0.67424 (7)	0.4291 (2)	0.17264 (5)	2.09 (2)	C15	0.93800 (12)	0.1313 (5)	0.10518 (9)	3.31 (4)
O4	0.68591 (8)	0.0401 (3)	0.14683 (6)	2.39 (3)	C16	0.88775 (13)	0.2746 (4)	0.11044 (9)	2.91 (4)
O5	0.78113 (7)	0.4168 (2)	0.24906 (5)	1.97 (2)	C21	0.63086 (9)	0.3659 (4)	0.13253 (7)	1.84 (3)
O6	0.68022 (10)	0.5211 (4)	0.02678 (7)	4.65 (4)	C22	0.63829 (10)	0.1531 (4)	0.11761 (7)	2.03 (3)
O7	0.82119 (12)	0.8237 (5)	0.04613 (8)	5.15 (5)	C23	0.59863 (12)	0.0801 (4)	0.07404 (8)	2.72 (4)
O8	0.92699 (9)	0.3448 (3)	0.26799 (7)	3.59 (4)	C24	0.54974 (13)	0.2146 (5)	0.04748 (9)	3.05 (5)
O9	0.98784 (9)	0.9327 (4)	0.29549 (7)	3.82 (4)	C25	0.54060 (12)	0.4178 (5)	0.06321 (9)	2.97 (4)
					C26	0.58144 (11)	0.4955 (4)	0.10611 (8)	2.38 (4)

^{a} $B_{eqv} = {}^4/_3[a^2\beta_{11} + b^2\beta_{22} + c^2\beta_{33} + ab(\cos\gamma)\beta_{12} + ac(\cos\beta)\beta_{13} + bc(\cos\alpha)\beta_{23}]$.

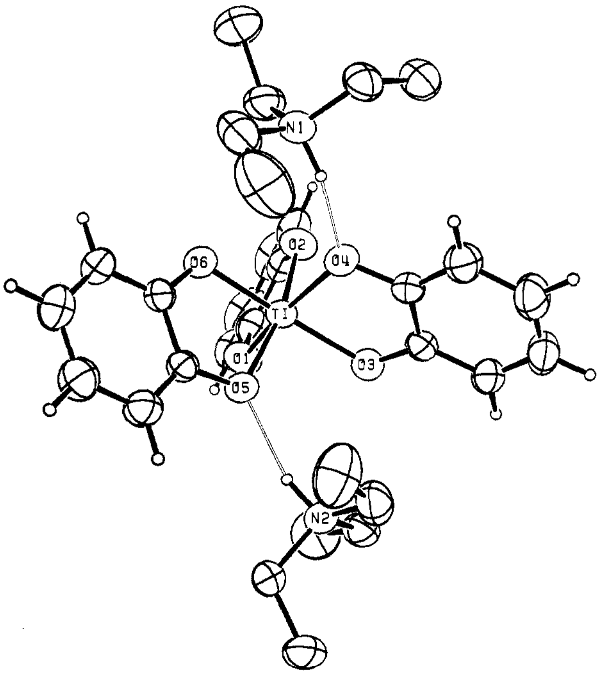

Figure 1. Molecular structure of the complex anion and its hydrogen bonding to the cation in $[Et_3NH]_2[Ti(cat)_3]$ (**2**).

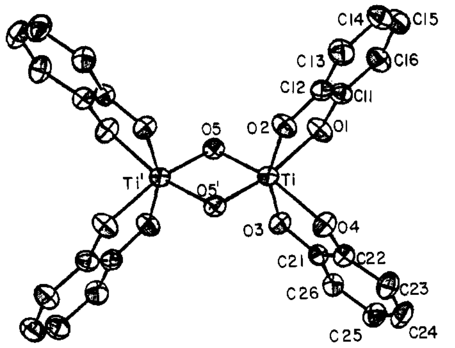

Figure 2. Molecular structure of the dimeric anion in $K_4[TiO(cat)_2]_2 \cdot 9H_2O$ (**4**).

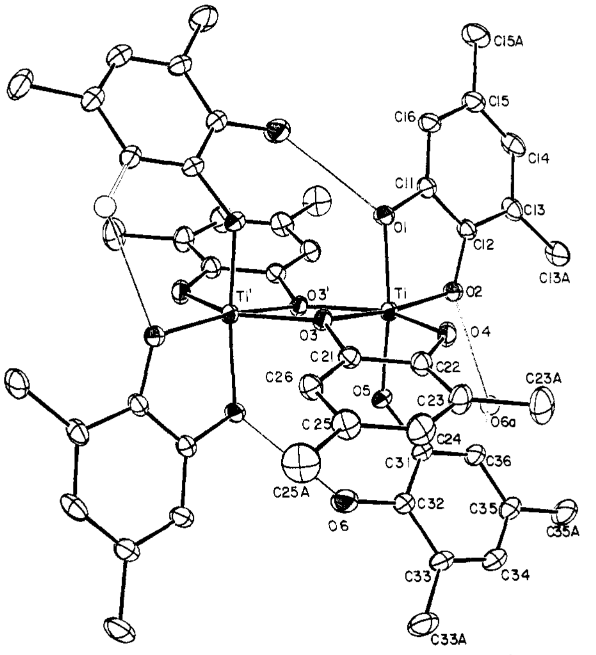

Figure 3. Molecular structure of the dimeric anion in $[Et_3NH]_2[Ti(DTBC)_2(HDTBC)]_2 \cdot 2CHCl_3$ (**5**). The location of the partially occupied protonated oxygen is indicated by the open bond and atom. Methyl carbons of the *tert*-butyl groups have been removed for clarity.

in the structure factor calculations. The hydrogen atoms at positions 4 and 6 and some of the hydrogen atoms for the cation and the *tert*-butyl groups in position 3 were located. All hydrogen atoms (including those not found in the difference Fourier) were placed at idealized coordinates with isotropic thermal factors ranging from 6 to 17 Å^2. Addition of the hydrogen atoms resulted in a large drop in the R factor since the 78 hydrogen atoms account for nearly 16% of F_{000} (500 e). With the p factor in the weighting scheme set to 0.06, the refinement converged to $R = 6.23\%$ and $R_w = 8.71\%$. The error in an observation of unit weight was 2.07 for 6722 observations and 541 variables. The maximum peak in the final difference map was 0.62 e/Å^3. Table VIII gives the positional and thermal parameters.[11]

Description of the Structures

Important bond distances and angles are summarized in Table XIV;[11] the structures and atom numbering schemes are shown in Figures 1–3.

$[Et_3NH]_2[Ti(cat)_3]$. The anion in **2** is a monomeric tris complex with only moderate deviations from octahedral geometry for the inner coordination sphere. The complete ion-pair complex possesses nearly twofold symmetry, as seen in Figure 1. Thus it has one unique and unexceptional catecholate ligand (O1···O2) and two ligands which are distorted by strong hydrogen bonds to the Et_3NH^+ cations (O4···N1 = 2.708 (2) Å, O5···N2 = 2.857 (2) Å). This H bonding is reflected in the lengthening of the associated Ti···O4, and Ti···O5 bonds, which average 0.05 Å longer than the unaffected bonds. This effect is similar to that previously observed in the analogous $[Et_3NH]_2[V(cat)_3]$ structure.[4] The trigonal twist angle, 43.5°, and the ligand bite distance, 2.537 Å, are in accord with the trends seen in other tris(catecholate) complexes, as these structural parameters vary with the size of the central ion.[4,12] As observed in the past,[4,12] the catechol ligands

---

(12) Raymond, K. N.; Isied, S. S.; Brown, L. D.; Fronczek, F. R.; Nibert, J. H. *J. Am. Chem. Soc.* **1976**, *98*, 1767.

Table VIII. Positional Parameters of $[Et_3NH]_2[Ti(DTBC)_2(HDTBC)]_2 \cdot 2CHCl_3$

atom	*x*	*y*	*z*	B_{eqv}, Å^{2a}
Ti	0.01821 (4)	−0.05571 (4)	0.12125 (4)	2.79 (1)
O1	0.1615 (2)	−0.1009 (2)	0.0982 (1)	3.38 (6)
O2	0.0620 (2)	−0.1790 (2)	0.2434 (1)	3.34 (5)
O3	−0.0061 (1)	0.0890 (1)	−0.0080 (1)	2.85 (5)
O4	−0.0007 (2)	0.0480 (2)	0.1675 (1)	3.77 (6)
O5	−0.1175 (2)	−0.0572 (2)	0.1417 (1)	3.53 (6)
O6	−0.2680 (2)	0.1325 (2)	0.0630 (2)	4.47 (8)
C11	0.2160 (2)	−0.1897 (2)	0.1752 (2)	3.37 (8)
C12	0.1613 (2)	−0.2315 (2)	0.2591 (2)	3.37 (8)
C13	0.2072 (3)	−0.3177 (3)	0.3469 (2)	3.94 (9)
C14	0.3096 (3)	−0.3644 (3)	0.3426 (3)	4.7 (1)
C15	0.3644 (3)	−0.3297 (3)	0.2585 (3)	4.6 (1)
C16	0.3169 (2)	−0.2394 (3)	0.1735 (2)	4.3 (1)
C13A	0.1487 (3)	−0.3554 (3)	0.4414 (3)	5.2 (1)
C13B	0.0961 (4)	−0.2603 (4)	0.4647 (3)	7.3 (2)
C13C	0.2166 (4)	−0.4442 (5)	0.5316 (3)	8.9 (2)
C13D	0.0748 (3)	−0.4012 (4)	0.4282 (3)	7.2 (2)
C15A	0.4751 (3)	−0.3913 (4)	0.2586 (3)	6.5 (1)
C15B	0.5276 (5)	−0.3329 (8)	0.1742 (7)	14.6 (4)
C15C	0.5252 (6)	−0.413 (1)	0.3464 (7)	25.3 (7)
C15D	0.4853 (7)	−0.4919 (7)	0.257 (1)	30.6 (5)
C21	−0.0510 (2)	0.1777 (2)	0.0086 (2)	3.15 (7)
C22	−0.0458 (2)	0.1540 (2)	0.1070 (2)	3.51 (8)
C23	−0.0847 (2)	0.2381 (3)	0.1353 (2)	4.56 (9)
C24	−0.1279 (3)	0.3412 (2)	0.0603 (3)	5.0 (1)
C25	−0.1352 (3)	0.3646 (3)	−0.0359 (3)	4.8 (1)
C26	−0.0958 (3)	0.2808 (2)	−0.0633 (2)	3.74 (8)
C23A	−0.0789 (4)	0.2162 (3)	0.2434 (3)	6.2 (1)
C23B	0.0297 (4)	0.1795 (4)	0.2709 (4)	9.9 (2)
C23C	−0.1316 (6)	0.3186 (4)	0.2568 (3)	11.3 (2)
C23D	−0.1236 (4)	0.1285 (4)	0.3117 (3)	8.3 (2)
C25A	−0.1844 (4)	0.4818 (3)	−0.1158 (3)	6.5 (1)
C25B	−0.2740 (8)	0.5385 (6)	−0.0707 (7)	14.4 (3)
C25C	−0.2225 (7)	0.4858 (5)	−0.2014 (5)	11.7 (3)
C25D	−0.1109 (7)	0.5436 (6)	−0.139 (1)	19.5 (5)
C31	−0.1874 (2)	−0.0308 (2)	0.2041 (2)	3.45 (8)
C32	−0.2641 (3)	0.0659 (3)	0.1624 (2)	4.11 (9)
C33	−0.3406 (3)	0.0943 (3)	0.2222 (3)	4.7 (1)
C34	−0.3365 (3)	0.0198 (3)	0.3204 (3)	5.1 (1)
C35	−0.2628 (3)	0.0775 (3)	0.3635 (3)	5.0 (1)
C36	−0.1859 (3)	0.1021 (3)	0.3034 (2)	4.13 (9)
C33A	−0.4255 (3)	0.2034 (3)	0.1793 (3)	6.2 (1)
C33B	−0.4940 (4)	0.2194 (4)	0.2601 (4)	10.1 (2)
C33C	−0.4882 (4)	0.2032 (5)	0.1061 (4)	8.7 (2)
C33D	−0.3847 (5)	0.2975 (4)	0.1266 (5)	10.4 (2)
C35A	−0.2628 (3)	−0.1573 (4)	0.4735 (3)	6.8 (1)
C35B	−0.3575 (6)	−0.1214 (9)	0.5229 (5)	13.9 (4)
C35C	−0.252 (1)	−0.2684 (7)	0.4833 (6)	17.9 (5)
C35D	−0.1772 (7)	−0.166 (1)	0.5248 (5)	15.3 (4)
N	−0.2087 (3)	−0.1672 (3)	0.0778 (3)	7.2 (1)
CN1	−0.1501 (5)	−0.2868 (5)	0.1303 (6)	14.0 (3)
CN2	−0.1226 (6)	−0.3251 (5)	0.2302 (5)	12.9 (3)
CN3	−0.2008 (4)	−0.1394 (4)	−0.0299 (5)	11.1 (2)
CN4	−0.2549 (5)	−0.1940 (5)	−0.0610 (5)	15.5 (2)
CN5	−0.3068 (5)	−0.1425 (5)	0.1122 (5)	13.4 (2)
CN6	−0.3676 (6)	−0.0321 (6)	0.0471 (8)	18.8 (4)
C	0.6517 (5)	0.1406 (5)	0.6432 (5)	11.2 (2)
Cl1	0.7617 (2)	0.0458 (2)	0.6670 (2)	17.0 (1)
Cl2	0.6247 (2)	0.2143 (2)	0.5179 (2)	17.2 (1)
Cl3	0.5585 (2)	0.0793 (2)	0.7010 (2)	17.5 (1)

[a] $B_{eqv} = {}^4/_3[a^2\beta_{11} + b^2\beta_{22} + c^2\beta_{33} + ab(\cos\gamma)\beta_{12} + ac(\cos\beta)\beta_{13} + bc(\cos\alpha)\beta_{23}]$.

are bent at the oxygen atoms, with the dihedral angles between the O–Ti–O and the aromatic ring planes being 5.7, 3.2, and 2.9° for ligands 1, 2, and 3, respectively.

$K_4[TiO(cat)_2]_2 \cdot 9H_2O$. Complex **4** is a dimer bridged by oxygen atoms with a center of inversion at the midpoint of the metal centers. The molecular symmetry is approximately C_{2h}. The four-membered ring thus formed is a lozenge, with internal angles of 82.01 (1)° at the metal and 98.0 (1)° at the oxygen atom. The Ti–O bonds trans to the bridging oxygens are much longer than the cis bonds, as would be expected from the structural trans influence of the oxide anions. The Ti···Ti distance is 2.819 (1) Å as compared with 2.719 (1) Å found in the structure of dimeric $[TiO(acac)_2]_2$[13] and 3.197 (3) Å reported for $[Ti(OEt)_2(CH_2Ph)_2]_2$.[14] The average O–Ti–O chelate angle is 78.1 (1)°, while the corresponding angle in the analogous oxovanadium complex is 82.8 (1)°.[4] The dihedral angles between the O–Ti–O and the aromatic ring planes are 3.4 and 11.0° for ligands 1 and 2, respectively. The potassium ions are coordinated by six oxygen atoms with K–O distances ranging from 2.6 to 3.1 Å. In contrast to the V(IV) complex, which contains the vanadyl moiety, is five-coordinate, and possesses approximate C_{2v} symmetry, the Ti(IV) ion forms a bis(μ-oxo) dimer. This is a consequence of the inherent stability of VO^{2+}, which arises from the energetic availability of the vanadium 3d orbitals for π donation from the axial oxygen. In titanium the 3d orbitals are higher in energy, so strong π bonding is not observed.

$[Et_3NH]_2[Ti(DTBC)_2(HDTBC)]_2 \cdot 2CHCl_3$. The coordination sphere about the metal centers in **5** consists of one catechol *monoanion* and two dianions. One of the bidentate catechol dianion oxygens is shared by both metal atoms. Because of this edge-sharing effect, the Ti–O (bridge) bonds are elongated by approximately 0.1 Å from normal values (for example, the axial Ti–O distances are 1.974 (2) Å for O1 and 1.936 (2) Å for O5) and the Ti–O3–C21 angle is small. In addition, the bridging catechol dianion is pulled in toward the center of the molecule, which causes a considerable decrease in the O3′–Ti–O4 angle (148.9 (1)° vs. 168.1 (1)° for the O2–Ti–O3 angle). The Ti···Ti′ distance is 3.326 (1) Å. In a similar catechol-bridged Fe(III) dimer,[15] the Fe···Fe distance was reported to be 3.15 Å. The free hydroxyl (O6) group of the monoanion is hydrogen bonded to O1′ (O1′···O6 = 2.861 (2) Å and O1′···O6–C32 = 132.3 (2)°). The intramolecular hydrogen bonding is shown in Figure 3. The Et_3NH^+ cation also forms an intermolecular hydrogen bond with O5 (N···O5 = 2.918 (3) Å). The catechol C–C distances do not show the usual long–short–long variation seen in other catecholate structures, which is ascribed to the disorder in the structure. Catechol ligands 1 and 2 are bent at the oxygen atoms with dihedral angles between the O–Ti–O and aromatic ring planes of 5.1 and 17.5°, respectively.

Physical Characterization and Properties

Infrared Spectra. The infrared spectra of $[NH_4]_2[Ti(cat)_3] \cdot 2H_2O$ (**1**), $K_4[TiO(cat)_2]_2 \cdot 2H_2O$ (**3**), and $[Et_3NH]_2[Ti(DTBC)_2(HDTBC)]_2 \cdot 2CHCl_3$ (**5**), tabulated in Table XIX, show the presence of catechol modes undergoing shifts typical of coordination to a metal ion.[16] In particular, ν(C=C) which occurs at 1585 cm^{-1} in free catechol appears as a band at 1562 cm^{-1} in the tris complex **1** and as bands at 1589 and 1567 cm^{-1} in dimer **3** and at 1582 and 1560 cm^{-1} in dimer **5**. Comparison of the IR spectra for the tris complex and dimer **3** shows that, apart from the N–H stretching region, the only significant difference between the two spectra is the band at 665 cm^{-1} in **3**. Bands in the 650–700-cm^{-1} region previously have been assigned[17,18] to M_2O_2 groups in bis(μ-oxo) Mn(III) and Mn-

---

(13) Smith, G. D.; Caughlan, C. N.; Campbell, J. A. *Inorg. Chem.* **1972**, *11*, 2989.

(14) Evans, M. S. *Helv. Chim. Acta* **1975**, *58*, 373.

(15) Anderson, B. F.; Buckingham, D. A.; Robertson, G. B.; Webb, J.; Murry, K. S.; Clark, P. E. *Nature (London)* **1976**, *262*, 722.

(16) Itoh, Y.; Nakahara, M.; Kondo, Y. *Nippon Kagaku Zasshi* **1971**, *92*, 227.

(17) Cooper, S. R.; Calvin, M. *J. Am. Chem. Soc.* **1977**, *99*, 6623.

Table XIV. Selected Distances (Å) and Angles (deg) with Chemically Equivalent Averages[a]

	$[Et_3NH]_2[Ti(cat)_3]$	$K_4[TiO(cat)_2]_2\cdot 9H_2O$		$[Et_3NH]_2[Ti(DTBC)_2(HDTBC)]_2\cdot 2CHCl_3$	
		Distances			
Ti-O1	1.941 (1)	Ti-O2	1.993 (1)	Ti-O1	1.974 (2)
Ti-O2	1.964 (1)	Ti-O3	1.987 (1)	Ti-O5	1.936 (2)
Ti-O3	1.933 (1)	av Ti-O_{axial}	1.990 (3)		1.955 (9)
Ti-O4	2.014 (1)	Ti-O1	2.032 (1)	Ti-O2	1.889 (2)
O5	1.986 (1)	Ti-O4	2.070 (1)	Ti-O2	1.885 (2)
O6	1.957 (1)	av Ti-O_{trans}	2.051 (9)		1.887 (2)
		Ti-O5	1.859 (1)	Ti-O3	2.079 (1)
		Ti-O5′	1.876 (1)	Ti-O3′	2.041 (2)
		av Ti-O_{bridge}	1.868 (9)		2.060 (19)
av Ti-O	1.966 (27)		1.970 (77)		1.967 (73)
O1-C11	1.339 (3)		1.338 (2)		1.354 (3)
O1-C12	1.345 (3)		1.350 (2)		1.367 (3)
O3-C21	1.344 (2)		1.339 (2)		1.372 (3)
O4-C22	1.349 (2)		1.337 (2)		1.353 (3)
O5-C31	1.353 (2)				1.373 (3)
O6-C32	1.338 (2)				1.368 (3)
av O-C	1.345 (3)		1.341 (5)		1.365 (8)
C11-C12	1.406 (3)		1.407 (2)		1.395 (3)
C21-C22	1.407 (3)		1.410 (2)		1.388 (3)
C31-C32	1.411 (2)				1.388 (3)
av C1-C2	1.408 (2)		1.409 (2)		1.390 (3)
C12-C13	1.377 (3)		1.384 (2)		1.393 (3)
C22-C23	1.388 (3)		1.395 (2)		1.408 (3)
C32-C33	1.381 (3)				1.409 (3)
C11-C16	1.377 (3)		1.396 (2)		1.390 (3)
C21-C26	1.379 (3)		1.385 (2)		1.376 (3)
C31-C36	1.378 (3)				1.384 (3)
av C2-C3	1.380 (4)		1.390 (6)		1.393 (12)
C13-C14	1.408 (5)		1.397 (2)		1.406 (4)
C23-C24	1.399 (3)		1.392 (2)		1.389 (4)
C33-C34	1.392 (3)				1.381 (4)
C16-C15	1.396 (5)		1.400 (2)		1.394 (3)
C26-C25	1.389 (3)		1.401 (2)		1.394 (4)
C36-C35	1.392 (3)				1.398 (3)
av C3-C4	1.396 (6)		1.398 (4)		1.394 (8)
C14-C15	1.372 (6)		1.372 (3)		1.381 (4)
C24-C25	1.368 (4)		1.368 (2)		1.361 (4)
C34-C35	1.369 (3)				1.373 (4)
av C4-C5	1.370 (2)		1.370 (2)		1.372 (8)
		Hydrogen Bonds			
O4-N1	2.708 (2)			O5-N	2.918 (3)
O5-N2	2.857 (2)			O6-O1′	2.861 (2)
				O6a-O2	2.737 (2)
		Angles			
O1-Ti-O2	80.6 (1)		78.1 (1)		79.6 (1)
O3-Ti-O4	80.1 (1)		78.1 (1)		77.5 (1)
O5-Ti-O6	80.3 (5)				
av ring cis O-Ti-O	80.3 (2)		78.1 (1)		78.6 (11)
O1-Ti-O4	167.9 (1)	O1-Ti-O5′	166.2 (1)	O1-Ti-O5	160.2 (1)
O2-Ti-O5	167.4 (1)	O2-Ti-O3	159.4 (1)	O2-Ti-O3	168.1 (1)
O3-Ti-O6	163.5 (1)	O4-Ti-O5	165.8 (1)	O3-Ti--O4	148.9 (1)
av trans O-Ti-O	166.3 (20)		163.8 (31)		159.1 (79)
Ti_2-O_2 ring					
Ti-O-Ti			98.0 (1)		107.6 (1)
O-Ti-O			82.0 (1)		72.4 (1)

[a] Standard deviations are calculated from the formula $\sigma(\bar{x}) = [(1/n(n-1))\Sigma_{i=1}{}^{n}(x_i - \bar{x})^2]^{1/2}$ or $\sigma(\bar{x}) = [\Sigma_{i=1}{}^{n} 1/\sigma_i{}^2]^{-1/2}$, whichever is greater.

(IV) complexes. The presence of the 665-cm^{-1} band in the bis(μ-oxo) dimer **3**, but not in the monomeric complex **1**, strongly suggests that this band *is* due to the Ti_2O_2 group. This band must originate from either the B_{2u} or B_{3u} ring modes of the M_2O_2 unit (assuming D_{2h} symmetry, with the Ti–Ti and O–O vectors along x and y, respectively). No definitive assignments of M_2O_2 vibrational spectra have been made. However, Nakamoto has compiled the vibrational assignments for M_2X_6 (D_{2h}) systems.[19] Of particular relevance here is the Al_2F_6 complex for which the B_{2u} and B_{3u} modes are assigned to bands at 600 and 575 cm^{-1}, respectively. On the basis of this assignment we could expect to see the B_{2u} and B_{3u} modes as two closely spaced bands between 600 and 700 cm^{-1}. In fact, the broad 665-cm^{-1} band may well be the superposition of both vibrations.

Optical Spectra. As previously reported,[7,20] the optical spectrum of $[NH_4]_2[Ti(cat)_3]$ (Figure 4) shows an intense

---

(18) Boucher, L. J.; Coe, C. G. *Inorg. Chem.* **1975**, *14*, 1289.

(19) Nakamoto, K. "Infrared and Raman Spectra of Inorganic and Coordination Compounds", 3rd ed.; Wiley: New York, 1978; p 165.

(20) Martin, J. L.; Takats, J. *Can. J. Chem.* **1975**, *53*, 572.

Table XIX. IR Data (cm^{-1}) (KBr Pellet)

$[NH_4]_2$-$[Ti(cat)_3]\cdot 2H_2O$	$K_4[TiO(cat)_2]_2\cdot 2H_2O$	$[Et_3NH]_2$-$[Ti(DTBC)_2$-$(HDTBC)]_2\cdot 2CHCl_3$
3555 s	3569 s	3340 m, b
3251 s	3400 s, b	2948 s
3140 m, b	3060 w	2900 m
2995 s, b	3004 w	2862 m
2820 s, b	1645 m	1582 m
1612 w	1589 m	1560 m
1562 m	1567 m	1475 s
1475 s	1475 s	1440 s
1446 s	1441 w	1411 s
1398 m	1324 m	1386 w
1331 m	1249 s	1357 m
1315 w	1219 w	1316 w
1247 s	1147 w	1292 s
1206 m	1095 m	1238 s
1096 m	1017 m	1214 m
1015 w	898 w	1200 m
903 w	863 m	1170 w
863 m	795 s	1153 w
798 s	745 s	1105 w
743 s	730 s	1023 w
626 s	665 s	978 s
597 s	615 s	910 w
503 m	598 s	859 m
408 m	491 s	831 s
311 m	480 s	812 m
	415 m	750 s
	345 m	732 m
	280 m	686 s
		620 s
		593 s
		542 w
		516 m
		502 m
		482 w
		467 w
		409 w

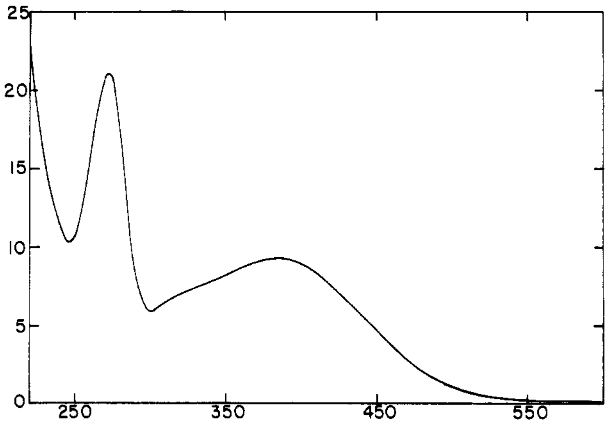

Figure 4. UV-vis spectrum of **1** in H_2O.

ligand to metal charge-transfer band with a maximum at 389 nm (ϵ 9300). The low-energy tail of this band accounts for the red color of the complex. No bands attributable to d–d transitions are observed, as expected for Ti(IV) (d^0). The optical spectrum of the tris complex is unchanged from pH 6 to pH 12, as is the electrochemical behavior (vide infra), even in the absence of excess catechol. This is in sharp contrast with the corresponding Fe(III) complex, which dissociates catechol upon lowering the pH from 9 to 7.[21] This increased stability of the tris complex is a consequence of the extreme acidity of Ti(IV).[7] However, in very basic solutions (above pH 12) reversible spectral changes appear that reflect the onset of hydrolysis to the bis(μ-oxo) dimer **3**. This reaction is essentially a ligand exchange between O^{2-} and the catechol dianion described by eq 1. The reaction is driven to the right

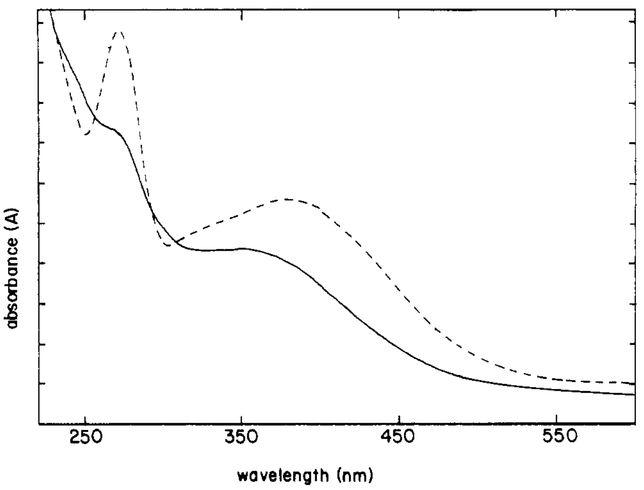

Figure 5. Solid-state UV-vis spectra of **1** (- - -) and **3** (—) in KBr. The absorbance scale is arbitrary.

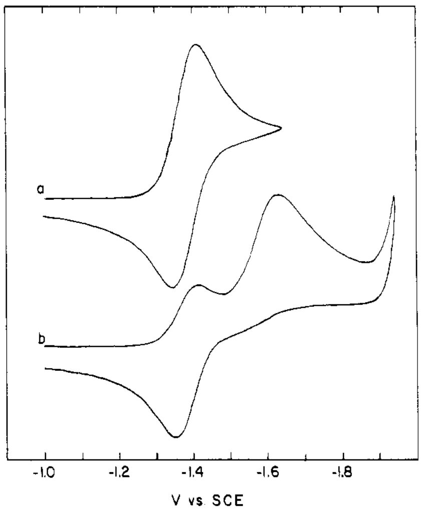

Figure 6. Cyclic voltammograms of **1**: (a) pH 7.83; (b) pH 13.40.

$$2Ti(cat)_3{}^{2-} + 2OH^- \rightleftharpoons [TiO(cat)_2]_2{}^{4-} + 2Hcat^- \quad (1)$$

only at high pH because of the large (≥0.1 M) concentration of OH^- then available. A reliable solution spectrum of dimer **3** could not be obtained due to the facile disproportionation reaction in dilute solution, shown by eq 2. An additional

$$[TiO(cat)_2]_2{}^{4-} + 2H_2O \rightleftharpoons Ti(cat)_3{}^{2-} + cat^{2-} + Ti(OH)_4 \quad (2)$$

difficulty may arise from the rapid oxidation of the free catechol dianion by residual oxygen. This oxidation is strongly favored under basic conditions and results in a thermodynamic sink which drives the reaction to the right. However, a solid-state spectrum of **3** was obtained in KBr and is shown in Figure 5 along with the solid-state spectrum of **1**.

Electrochemistry. Cyclic voltammetry performed on the tris complex, **1**, in 1 M KCl reveals a reversible one-electron-reduction wave with $E_f = -1.38$ V vs. SCE, a peak separation of 65 mV, and a peak current ratio of 1.06 (Figure 6a). The cyclic voltammetric behavior is constant over the pH range 6–12, consistent with the optical results. From the reversibility of the couple it may be inferred that not only the Ti(IV) but also the Ti(III) tris complex is fully formed in the pH range 6–12. Coulometric measurements verified the one-electron

---

[21] Avdeef, A.; Sofen, S. R.; Bregante, T. L.; Raymond, K. N. *J. Am. Chem. Soc.* **1978**, *100*, 5362.

stoichiometry of this reduction and yielded a pale green solution of $[Ti^{III}(cat)_3]^{3-}$.

Above pH 13 the reddish titanium(IV) tris(catecholate) solution reversibly changes to a clear yellow solution (vide supra) with concomitant changes in electrochemical behavior. These changes involve a decrease in current of the reversible $Ti^{IV/III}(cat)_3$ wave at −1.38 V, and the appearance of a new, irreversible wave at −1.62 V, which grows with increasing pH (Figure 6b). When the pH is raised still further, the new wave approaches reversibility, as judged by peak separation. However, it did not prove possible to obtain fully reversible behavior. Previous workers[20] were puzzled that no reduction waves were apparent on polarographic examination of $[Et_4N]_2[Ti(cat)_3]$ in CH_2Cl_2 or CH_3CN. Unless the solvent exhibits a profound effect on this reduction, we are unable to account for this reported lack of reduction.[22] Both the changes in electrochemical behavior and the optical spectrum are reversible with pH. It may be inferred that the high pH process involves loss of a catechol to yield the bis(μ-oxo) dimer since addition of catechol raises the pH value at which the onset of irreversibility occurs.

Conclusion

The structural aspects of this work show that, while the Ti(IV)–catechol affinity is very high, the very hard-acid nature of Ti(IV) gives rise to more complicated equilibria than seen in the first-row M(III) ions. Under very basic conditions Ti(IV) is capable of stabilizing the oxide anion, and ligand exchange occurs to yield the bis(μ-oxo) dimer $[TiO(cat)_2]_2^{4-}$. Conversely, Ti(IV) is better able to stabilize the cat^{2-} anion under acidic conditions than Fe(III). This is manifested both in the large pH stability range of the tris complex (pH 6–12) and in the existence of the dimeric complex **5**. Here protonation of a catechol results not in dissociation yielding the bis complex but rather in catechol oxygen bridging to yield the dimeric $[Ti(DTBC)_2(HDTBC)]_2^{2-}$ complex. Thus the singly protonated catechol coordinates as a monodentate phenolate anion, and one of the catecholate dianion oxygen atoms bridges the metal ions to complete the coordination spheres. While it is probable that this protonated dimer does not persist in aqueous solution, this protonated phenolate mode of binding may be relevant to the coordination geometries proposed for the ferric ion containing catechol oxygenase enzymes. A five-coordinate Fe(III) model of such binding has recently appeared.[23]

The present study of the Ti(IV)–catechol complex chemistry underscores the remarkable facility of catechol to bind and stabilize metals in high oxidation states. Like ferric ion, Ti(IV) exhibits a high charge/radius ratio and as a consequence is exceedingly prone to hydrolysis. In the presence of catechol, however, the onset of Ti(IV) hydrolysis is shifted from approximately pH 1 to pH 13! Similarly, while the formal potential in acid for the Ti(IV)/Ti(III) couple is slightly positive (+0.099 V vs. NHE), this potential is shifted to −1.14 V vs. NHE for the $[Ti^{IV/III}(cat)_3]$ couple. The extremely low reduction potential of $[Ti^{IV}(cat)_3]^{2-}$ reflects the extent to which catechol prefers Ti(IV) to Ti(III) coordination. Consider the expression[24]

$$E_c - E_s = (-0.059/n)[\log (\beta_{IV}/\beta_{III})] \tag{3}$$

where β_{IV} and β_{III} are the stability constants for the reactions as defined in eq 4 and 5 and E_c and E_s are the potentials for

$$Ti^{3+} + 3cat^{2-} \rightleftharpoons Ti(cat)_3^{3-} \qquad \beta_{III} \tag{4}$$

$$Ti(OH)_2^{2+} + 2H^+ + 3cat^{2-} \rightleftharpoons Ti(cat)_3^{2-} + 2H_2O \qquad \beta_{IV} \tag{5}$$

the complex ion and the aqueous ion half-cells (eq 6 and 7),

$$Ti^{IV}(cat)_3^{2-} + e^- \rightleftharpoons Ti^{III}(cat)_3^{3-} \qquad E_c = -1.14 \text{ V (NHE)} \tag{6}$$

$$Ti(OH)_2^{2+} + 2H^+ + e^- \rightleftharpoons Ti^{3+} + H_2O \qquad E_s = +0.099 \text{ V (NHE)} \tag{7}$$

and n (=1) is the number of electrons involved in the redox system. The observed potential shift corresponds to a ratio of the formation constants $\beta_{IV}/\beta_{III} = 1 \times 10^{21}$. Using Sommer's value for β_{IV}, $10^{60.3}$ (adjusted by assuming that $pK_{a1} = 9.23$ and $pK_{a2} = 13.0$ for catechol), we find that $\beta_{III} \simeq 10^{40}$. This value is comparable to that for Fe(III), as expected from the similarity of the ionic radii for Fe(III) and Ti(III). The stabilities of both the Ti(IV) and Ti(III) tris(catecholates) suggest that an effective determination for Ti may be obtained by voltammetry under moderately alkaline conditions rather than the acidic conditions currently used.

Acknowledgment. This research has been supported by NIH Grant AI 11744 and partially by NIH Grant HL 24775. The Berkeley CHEXRAY facility was established in part from an NSF departmental instrumentation grant. We thank Dr. Fred Hollander for helpful discussions concerning crystallographic details.

Registry No. **1**, 88932-89-2; **2**, 88916-41-0; **3**, 88916-42-1; **4**, 88916-43-2; **5**, 88916-45-4; **5**·$2CHCl_3$, 88932-92-7.

Supplementary Material Available: Anisotropic thermal parameters of **2**, **4**, and **5** (Tables III, VI, and IX), assigned positional and thermal parameters of the hydrogen atoms of **2**, **4**, and **5** (Tables IV, VII, and X—including some disordered atoms in the latter), structure factor amplitudes of **2**, **4**, and **5** (Tables XI, XII, and XIII), additional bond lengths and angles for **2**, **4**, and **5** (Table XV), and least-squares planes for **2**, **4**, and **5** (Tables XVI, XVII, and XVIII) (122 pages). Ordering information is given on any current masthead page.

---

[22] In addition to coulometry, the following methods have been unsuccessfully tried to prepare the Ti(III) complex. (1) Use of $TiCl_3$ (purple crystals) as the starting material: To an aqueous solution of 1 equiv of $TiCl_3$ was added an ammoniacal solution (15%) of 3 equiv of catechol. Initially, the solution turned dark. Within a minute or so, there appeared a mixed green and red mass, which instantaneously turned red on warming with evolution of a gas (presumably H_2). Use of toluene as the solvent and Et_3N as the base resulted in an oily red material, from which red crystals separated out on standing. (2) Use of reducing agents: (a) A THF (distilled from CaH_2) solution of $[Et_3NH]_2[Ti(cat)_3]$ was stirred for 2 days over 50% Zn(Hg). No visual change in color was observed—no reaction. (b) Reduction of a THF solution of $[Et_3NH]_2[Ti(cat)_3]$ over 5% Na(Hg) yielded a mixture of light yellow and faint green compounds (insoluble in THF), which decomposed on exposure to air, first to a green compound and then to a brown mass. (c) A stirred solution of $[Et_3NH]_2[Ti(cat)_3]$ with $NaBH_4$ in THF gave an insoluble, air-stable yellow compound, the nature of which is unknown.

[23] Heistand, R. H., II; Roe, A. L.; Que, L., Jr. *Inorg. Chem.* **1982**, *21*, 676.

[24] Meites, L. "Polarographic Techniques"; Wiley: New York, 1965; p 279.